SAND95-0324C

Conf-9503116--1

ASSESSING ALTERNATIVE CONCEPTUAL MODELS OF FRACTURE FLOW

Clifford K. Ho
Sandia National Laboratories
P.O. Box 5800, MS-1324
Albuquerque, NM 87185-1324
(505) 848-0712

Abstract

The numerical code TOUGH2 was used to assess alternative conceptual models of fracture flow. The models that were considered included the equivalent continuum model (ECM) and the dual permeability (DK) model. A one-dimensional, layered, unsaturated domain was studied with a saturated bottom boundary and a constant infiltration at the top boundary. Two different infiltration rates were used in the studies. In addition, the connection areas between the fracture and matrix elements in the dual permeability model were varied. Results showed that the two conceptual models of fracture flow produced different saturation and velocity profiles—even under steady-state conditions. The magnitudes of the discrepancies were sensitive to two parameters that affected the flux between the fractures and matrix in the dual permeability model: 1) the fracture-matrix connection areas and 2) the capillary pressure gradients between the fracture and matrix elements.

Introduction

The possibility of fast-flow pathways in fractured unsaturated rock has received much attention lately, especially in nuclear waste management. The transport of radionuclides from buried nuclear waste packages can be enhanced if fast-flow paths exist in the surrounding environment. Such conditions may exist in the variably welded tuff units at the potential repository site at Yucca Mountain, Nevada. The ability to model the flow and transport in these systems is necessary to accurately assess the performance of the potential repository. However, the inability to accurately characterize fracture networks in situ and the lack of rigorous discrete fracture flow models has prompted the need for alternative conceptual models of fracture flow. Two of these models include the equivalent continuum model (ECM) and the dual permeability (DK) model.

The equivalent continuum model has been described in detail by Klavetter and Peters (1986) and Dudley et al. (1988). This model has been used extensively in describing flow through fractured rock as a result of its relative simplicity and ease of computational implementation. In this model, the pressures in the matrix and fractures are assumed equal. As a result, the flow through this fracture-matrix system is equivalent to flow through a composite porous medium, which has hydraulic properties comprised of both fractures and matrix properties. Dudley et al. express that for conditions similar to those found at Yucca Mountain (i.e. low infiltration rates and good coupling between the fracture and matrix), the equivalent continuum model provides a reasonable approximation to fracture-matrix flow. However, recent studies have shown that flow processes such as fingering in fractures (Glass and Tidwell, 1991) and mechanical aspects such as fracture coatings may effectively reduce the coupling between the fractures and matrix. This may cause pressure disequilibrium between the fractures and matrix, even under low infiltration rates.

If pressure equilibrium cannot be assumed, other models such as the dual permeability model must be used. Details of the dual permeability model can be found in Pruess and Narasimhan (1985) and Pruess (1983). Unlike the equivalent continuum model, the dual permeability model represents the fractures and matrix as separate continua. As a result, different pressures can exist in the fractures and matrix, which allows flow to occur between the two continua. Propagation of flow in fractures is more likely to be observed in these models, depending on such parameters as fracture-matrix conductance and capillary pressure gradients between the fractures and matrix. However, relatively few analyses have been performed with the dual permeability model in conjunction with analyzing fast flow paths for the assessment of a potential nuclear waste repository.

The purpose of this report is to compare the dual permeability and equivalent continuum models by simulating infiltration and flow through a one-dimensional, unsaturated, heterogeneous, fractured rock (the context being relevant to the potential

MASTER

DISCLAIMER

Portions of this document may be illegible in electronic image products. Images are produced from the best available original document.

nuclear waste repository at Yucca Mountain). Saturations and velocities resulting from the two models are compared, and sensitivity analyses are performed. Parameters such as the infiltration rate and the connection area between the fractures and matrix are varied to demonstrate the importance of specific variables on the resulting saturation and velocity profiles.

Numerical Approach

In order to compare the equivalent continuum and dual permeability models, infiltration into a hypothetical one-dimensional vertical transect of Yucca Mountain was investigated. Figure 1 shows a sketch of the domain that was modeled using TOUGH2 (1991). A saturated boundary condition was assumed at the bottom, and a constant infiltration rate was assumed at the top boundary. In the equivalent continuum model, 106 elements were used as shown in Figure 1. In the dual permeability model, an additional set of elements was created using MINC (Pruess, 1983) so that both the fracture and matrix continua could be modeled discretely. As a result, twice as many elements were used in the dual permeability model. In addition, the constant infiltration rate was applied only to the top of the fracture continuum in the dual permeability model. The material properties that were used for both models were taken from TSPA-93 (Wilson et al., 1994) and are summarized in Table 1. The van Genuchten (1980) capillary pressure and relative permeability curves were used for all calculations, and the initial saturation of all domain elements was set to 0.85. Isothermal conditions were assumed to exist, and the single-phase EOS9 module (Richard's equation) of TOUGH2 was used.

Parameters such as the fracture-matrix connection areas and the distances between the fractures and matrix that were used in the dual permeability model were calculated in MINC, part of the TOUGH2 code. Table 2 summarizes the important mesh-related parameters that were used in the dual permeability model for this study. Since MINC, in general,

Figure 1. One-dimensional layered model used in TOUGH2 simulations. The initial saturation of all the elements was set to 0.85.

calculates these parameters based on the geometry of an idealized set of fractures and matrix blocks, non-ideal physical features and processes such as fracture coatings and fingering may alter the value of these parameters. As a sensitivity analysis, the connection areas between the fracture and matrix elements (A_{f-m}) were reduced by two orders of magnitude from the MINC-calculated values in some of the dual permeability simulations. Other parameters, such as the distance between the fracture and matrix elements, could also have been varied, but the desired effect of reducing the conductance between the fracture and matrix elements would have been the same. The TOUGH2 simulations that were performed are summarized in Table 3. Each of the simulations was run until steady-state conditions were achieved. The runs were stopped at either a simulation time of one billion years or 4000 time steps, whichever came first.

Results

Infiltration Rate, q = 0.1 mm/year (Runs 1, 2, and 3)

Figure 2 shows the steady-state matrix saturations for the equivalent continuum and dual permeability models using an infiltration rate of 0.1 mm/year (3.16e-8 kg/sec). At this infiltration rate, the matrix elements were capable of conducting the entire flow. As a result, the saturations were less than one everywhere, and the saturations decreased in the non-welded units where the porosity was greater. The dual permeability model that used the MINC-calculated fracture-matrix connection areas produced saturations that were nearly identical to the saturations of the equivalent continuum model. This implies that the conductance between the fractures and matrix elements in the dual permeability model was sufficient to allow most of the liquid to be imbibed into the matrix where it was conducted through the matrix continuum. This is also shown in Figure 3(a), in which the fracture and matrix pore velocities are plotted. For reference, the composite pore velocity of the equivalent continuum model is also plotted. The matrix velocity is seen to be over six orders of magnitude larger than the fracture velocity for the MINC-calculated dual permeability model.
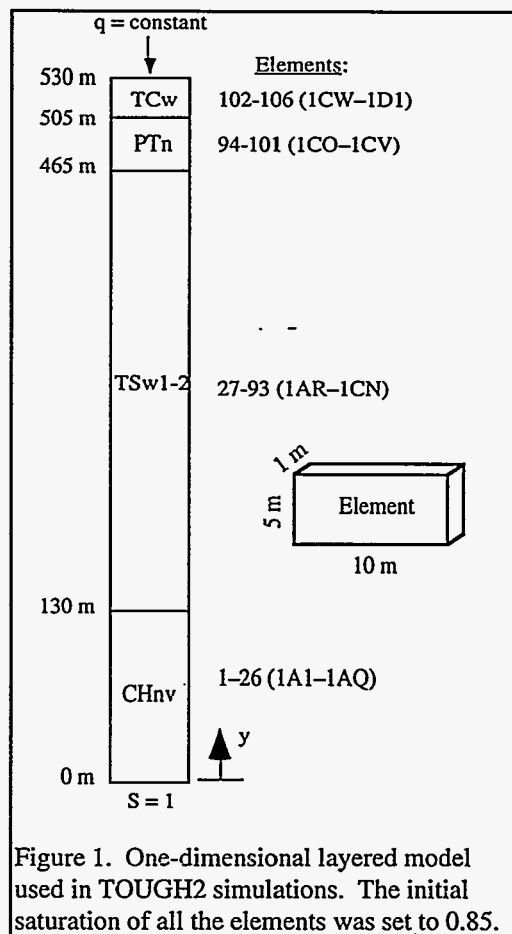
Table 1. TSPA93 (Wilson et al., 1994) parameters used in the TOUGH2 calculations.

	TCw	PTn[†]	TSw1-2	CHnv
Matrix				
porosity (m^3-p/m^3-m)	0.087	0.421	0.139	0.331
permeability (m^2)	2.04e-18	2.51e-14	2.09e-18	1.10e-16
α (1/Pa)	7.91e-7	3.78e-5	1.36e-6	2.79e-6
$\lambda = 1-1/\beta$	0.383	0.578	0.444	0.594
S_r	0.0212	0.154	0.0453	0.0968
S_s	1.0	1.0	1.0	1.0
Fracture				
porosity[††]	2.93e-4	9.27e-5	2.43e-4	1.11e-4
intrinsic perm. (m^2)	4.06e-9	7.14e-9	4.57e-9	6.53e-9
fracture spacing (m)	0.618	2.22	0.74	1.62
fracture aperture (m)	1.81e-4	2.06e-4	1.80e-4	1.79e-4
scaled perm. (m^2)	1.19e-12	6.62e-13	1.11e-12	7.23e-13
α (1/Pa)	1.23e-3	1.4e-3	1.22e-3	1.22e-3
$\lambda = 1-1/\beta$	0.667	0.667	0.667	0.667
S_r[†††]	0.0	0.0	0.0	0.0
S_s	1.0	1.0	1.0	1.0
Composite				
porosity	0.0873	0.421	0.139	0.331
permeability (m^2)	1.19e-12	6.87e-13	1.11e-12	7.23e-13

[†]The matrix permeability and α of the PTn were bi-modal, so the area weighted average was used for those parameters.

[††]The fracture porosity was calculated as the fracture aperture divided by the fracture spacing.

[†††]The residual fracture saturation was changed to 0.03 in the 0.1 mm/year infiltration cases because Run 2 could not reach steady-state within 4000 time steps using S_r=0.

Table 2. MINC (Pruess, 1983) input and output parameters for a 1-D dual permeability model with two interacting continua (fracture and 1 matrix continua).

	TCw	PTn	TSw1-2	CHnv
Aperture, b (m)	1.81e-4	2.06e-4	1.80e-4	1.79e-4
Fracture spacing, D (m^3)	0.62	2.2	0.74	1.6
Volume of grid block, V (m^3)	50	50	50	50
Fracture porosity, ϕ_f (b/D)	2.93e-4	9.27e-5	2.43e-4	1.11e-4
Fracture volume in grid block ($V*\phi_f$) (m^3)	1.46e-2	4.68e-3	1.22e-2	5.59e-3
Matrix volume in grid block ($V*(1-\phi_f)$) (m^3)	49.9854	49.9953	49.9878	49.9944
Distance between fracture and matrix, d=(D-b)/6 (m)	0.1033	0.3667	0.1233	0.2667
No. of matrix blocks per grid block, σ (V/D^3)	210	4.70	123	12.2
Fracture-matrix connection area on matrix block scale, $A'_{f-m}=2*(D-b)^2$ (m^2)	0.768	0.968	1.09	5.12
Fracture-matrix connection area on grid block scale, $A_{f-m}=A'_{f-m}*\sigma$ (m^2)	161	45.5	135	62.5

Table 3. Summary of TOUGH2 runs using the effective continuum model (ECM) and the dual permeability (DK) model.

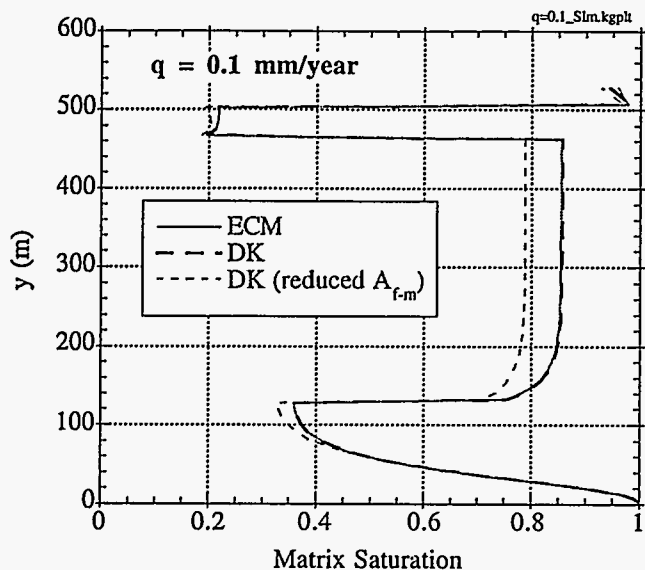| Run	q (mm/year)	model	comments
1	0.1	ECM	—
2	0.1	DK	—
3	0.1	DK	A_{f-m} reduced by 2 orders of magnitude
4	4.0	ECM	—
5	4.0	DK	—
6	4.0	DK	A_{f-m} reduced by 2 orders of magnitude

Figure 2. Steady-state matrix saturations for the equivalent continuum model (ECM), the dual permeability (DK) model as calculated by MINC, and a modified dual permeability model in which the fracture-matrix connection area was reduced by two orders of magnitude. The infiltration rate is 0.1 mm/year (3.16e-8 kg/sec).

However, when the connection area between the fractures and matrix (A_{f-m}) was reduced by two orders of magnitude, drastic changes were observed. Figure 2 shows that the matrix saturations for the modified dual permeability model were lower than the saturations of the previous models. The reduced conductance between the fractures and matrix reduced the flow to the matrix elements. The reduced flow through the matrix elements resulted in a decrease in the matrix saturations, which in turn increased the matrix capillary pressures. Although this caused an increase in the capillary pressure gradient between the fractures and matrix, the decreased fracture-matrix connection area offset the increased capillary pressure gradient. The end result was a larger portion of liquid flowing through the fractures. Figure 3(b) shows that the fracture pore velocities increased over six orders of magnitude from the previous dual permeability calculation, exceeding the matrix pore velocities.
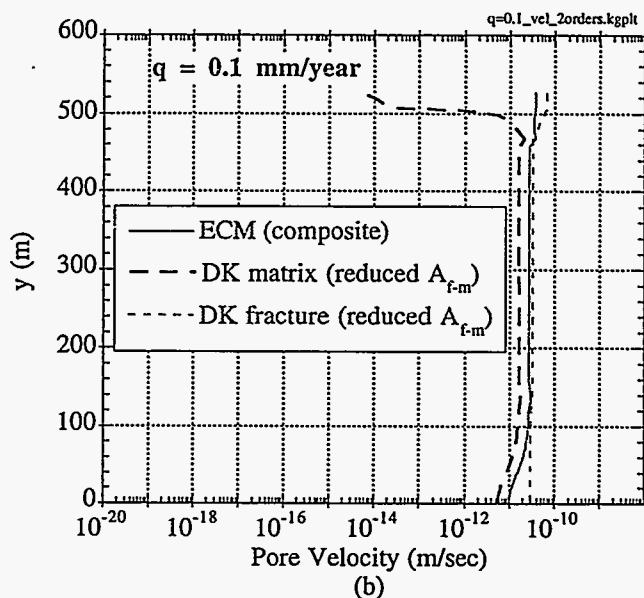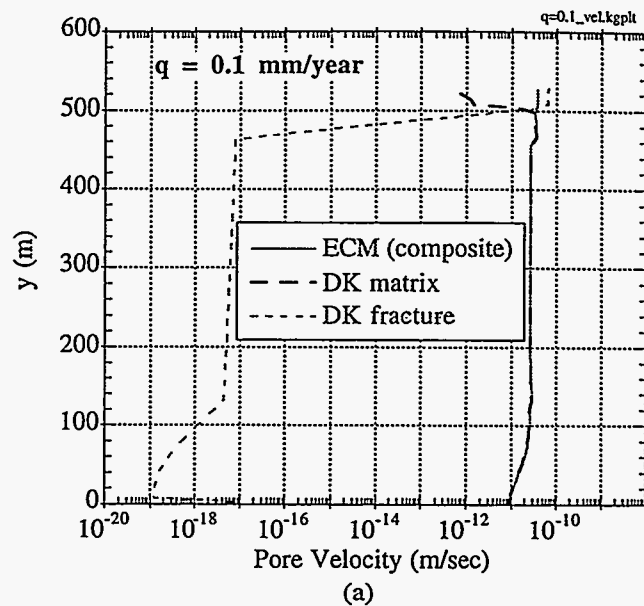

(a)

(b)

Figure 3. Steady-state pore velocities in the fractures and matrix: a) MINC-calculated dual permeability model; b) modified dual permeability model where the fracture-matrix area was reduced by two orders of magnitude. The composite ECM velocity is shown for reference. The infiltration rate is 0.1 mm/year (3.16e-8 kg/sec).

Infiltration Rate, q = 4.0 mm/year (Runs 4, 5, and 6)

At an infiltration rate of 4.0 mm/year, the saturated conductivities of the welded units (TCw and TSw1-2) were exceeded. As a result, Figure 4 shows that the steady-state saturations in the matrix of the welded units were nearly saturated for all the models. In the non-welded units (PTn and CHnv), the modified dual permeability model (in which the fracture-matrix connection area was reduced by two orders of magnitude) showed a decrease in the saturations. Note also that the MINC-calculated dual permeability model produced discrepancies from the equivalent continuum saturations at the top of the CHnv (y ~ 130 m). Since the flow was predominantly in the fractures through the welded TSw1-2 unit, the flow continued through the fractures even as it entered the non-welded CHnv unit.
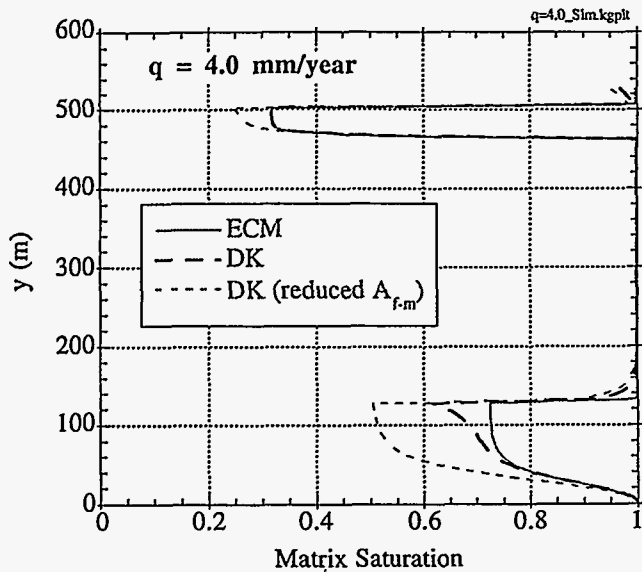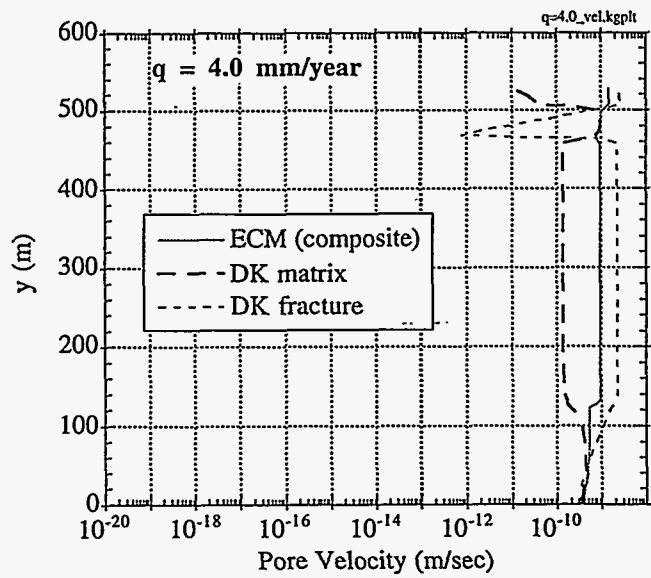
4

Figure 4. Steady-state matrix saturations for the equivalent continuum model (ECM), the dual permeability (DK) model as calculated by MINC, and a modified dual permeability model in which the fracture-matrix connection area was reduced by two orders of magnitude. The infiltration rate is 4.0 mm/year (1.266e-6 kg/sec).
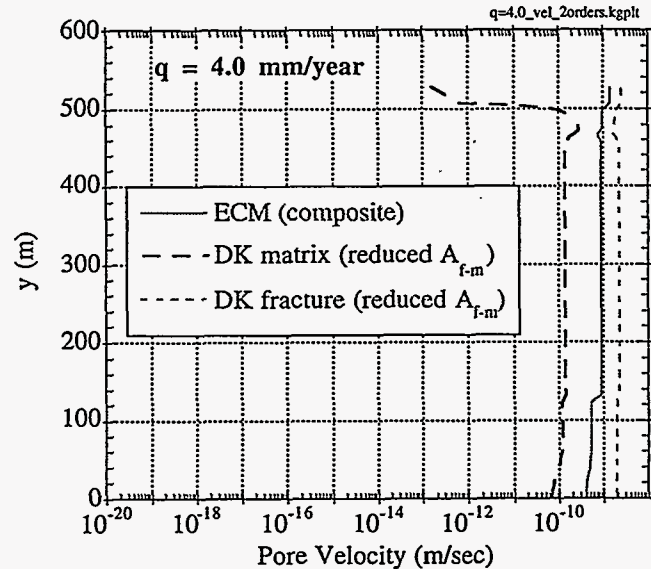
Figure 5(a) shows the fracture and matrix pore velocities for the MINC-calculated dual permeability model. The fracture velocities were higher than the matrix velocities in the welded TCw and TSw1-2 units, but the opposite was true in the non-welded PTn and CHnv units. Again, in this model the conductance between the fractures and matrix was large enough so that in regions where the matrix was not saturated (i.e. in units where the infiltration rate did not exceed the saturated conductivity), the flow was imbibed and subsequently carried by the matrix. However, the modified dual permeability model showed that by reducing the conductance between the fractures and matrix, the flow could remain in the fractures in regions where the matrix saturations were less than one. Figure 5(b) shows that in the modified dual permeability model the fracture velocities increased in regions where matrix flow dominated prior to the reduction in the fracture-matrix connection area. However, in the welded TCw and TSw1-2 units, where the matrix was saturated and fracture flow dominated from the onset, no changes in the velocity profiles were observed.
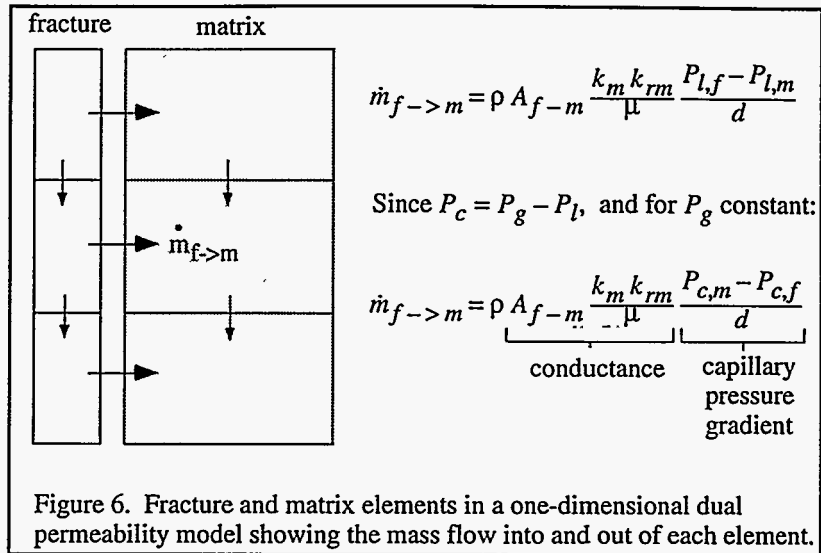

(a)

(b)

Figure 5. Steady-state pore velocities in the fractures and matrix: a) MINC-calculated dual permeability model; b) modified dual permeability model where the fracture-matrix area was reduced by two orders of magnitude. The composite ECM velocity is shown for reference. The infiltration rate is 4.0 mm/year (1.266e-6 kg/sec).

Discussion

In these numerical simulations, the dual permeability model was seen to produce similar results to the equivalent continuum model when the conductance between the fractures and matrix was sufficiently large. Since the MINC calculations were based on idealized geometric configurations of fracture and matrix blocks, the calculated conductance could be significantly different from that of actual systems. When this conductance was reduced by two orders of magnitude, the dual permeability model showed significant differences in the fracture and matrix velocities—even at steady-state. Intuitively, it

makes sense that *transient* responses to an infiltration event would be different if the fracture-matrix conductivity is altered, but the behavior of dual permeability systems under steady-state conditions is perhaps not so intuitive. Figure 6 shows a few elements from the one-dimensional dual permeability model used in this study. Figure 6 also shows Darcy's law as applied to the flow between a fracture and a matrix element. At steady-state, the mass flow into any element must equal the mass flow out of that element. If the connection area between the fracture and matrix (or any other parameters related to the conductance) is reduced, the mass flow rate into the matrix is also lowered. As long as this reduced mass flow into the matrix element equals the mass flow out of that element, steady-state conditions can be maintained. The result is a larger mass flow rate through the fractures.

$$\dot{m}_{f->m} = \rho\, A_{f-m} \frac{k_m k_{rm}}{\mu} \frac{P_{l,f} - P_{l,m}}{d}$$

Since $P_c = P_g - P_l$, and for P_g constant:

$$\dot{m}_{f->m} = \rho\, A_{f-m} \underbrace{\frac{k_m k_{rm}}{\mu}}_{\text{conductance}} \underbrace{\frac{P_{c,m} - P_{c,f}}{d}}_{\substack{\text{capillary}\\ \text{pressure}\\ \text{gradient}}}$$

Figure 6. Fracture and matrix elements in a one-dimensional dual permeability model showing the mass flow into and out of each element.

Note that in addition to the conductance terms of Darcy's law, the capillary pressure gradient between the fracture and matrix element also contributes to the mass flow into the matrix element. This explains why the 4.0 mm/year infiltration cases did not result in a change in the matrix saturations or velocities for the different models. At that infiltration rate, the capillary pressure of the fracture elements remained small due to higher fracture saturations. As a result of the large capillary pressure gradient, imbibition into the matrix elements continued until the matrix was nearly filled. In the 0.1 mm/year infiltration case, however, lower fracture saturations resulted in higher fracture capillary pressures, which reduced the capillary pressure gradient between the fractures and matrix. In both cases, the end result was based on the steady-state condition that the mass flow into an element equaled the mass flow out, where the mass flow rates between the fractures and matrix depended on both the conductance terms (e.g. fracture-matrix connection area) and the capillary pressure gradient.

Although the reduction in the connection area between the fracture and matrix elements seems arbitrary, physical processes and features observed in laboratory and field studies support this assumption in actual systems. Commonly observed flow channeling (or fingering) in fractures (Glass and Tidwell, 1991) and fracture coatings can act to effectively reduce the conductance between a fracture and matrix. When this occurs, both the physical observations and the numerical studies presented here show that the flow velocities through the fracture network can be significantly higher than the velocities that would be observed through either an effective continuum model or a dual permeability model based on idealized geometric configurations.

Finally, Table 4 shows the calculation times for each of the runs. The equivalent continuum simulations ran the fastest. Of the dual permeability runs, the ones with the reduced fracture-matrix connection area reached steady-state considerably faster than the MINC-calculated dual permeability models.

Table 4. Calculation times for TOUGH2 runs.

Run	No. of time steps	Simulated time (sec)	Calculation time (sec)
1	473	3.1536e16	89.8
2	4000	3.84e14	1615
3	393	3.1536e16	142
4	439	3.1536e16	87.1
5	4000	4.92e15	1772
6	981	3.1536e16	386

6

Conclusions

The equivalent continuum and dual permeability models were compared using TOUGH2. Infiltration into a one-dimensional, layered, unsaturated domain was investigated. The connection areas between the fractures and matrix were reduced by two orders of magnitude in some of the dual permeability runs as sensitivity analyses. Two different infiltration rates (0.1 mm/year and 4.0 mm/year) were used. Based on the results of these simulations, the following conclusions were drawn:

- The MINC-calculated dual permeability model (based on an ideal fracture-matrix geometry) produced similar results to those of the equivalent continuum model for both infiltration rates under steady-state conditions. For the 0.1 mm/year infiltration rate, the matrix was able to carry the entire flow. The 4.0 mm/year infiltration rate was greater than the saturated conductivity of the welded TCw and TSw1-2 units, which resulted in significant fracture flow in those regions.

- Reducing the conductance by two orders of magnitude between the fractures and matrix in the dual permeability model resulted in significantly higher fracture pore velocities where the matrix was unsaturated. Thus, depending on the fracture-matrix conductance, the dual permeability model is capable of modeling significant fracture propagation even when the matrix is unsaturated.

- The steady-state saturations and velocity profiles in the dual permeability model are sensitive to the fracture-matrix interaction. The fracture-matrix interaction depends on both the conductance terms between the fractures and matrix (e.g. the fracture-matrix connection area) and the capillary pressure gradient (which, in this study, was affected by the infiltration rates).

- The effective area (conductance) between fractures and matrix needs to be quantified and assessed through laboratory or field studies to provide reasonable estimates for use with the dual permeability model.

Nomenclature

A_{f-m}	connection area between the fracture and matrix elements
CHnv	Calico Hills non-welded vitric unit at Yucca Mountain
d	distance used to calculate fracture-matrix pressure gradients
DK	dual permeability
ECM	equivalent continuum model
k	permeability (m^2)
k_r	relative permeability
$m_{f->m}$	mass flow from the fracture to the matrix (kg/sec)
MINC	Multiple INteracting Continua (part of TOUGH2 code to generate dual permeability models)
P_c	capillary pressure (Pa)
P_g	gas pressure (Pa)
P_l	liquid pressure (Pa)
PTn	Paintbrush non-welded unit at Yucca Mountain
q	infiltration rate (mm/year)
S	liquid saturation
S_r	residual liquid saturation
S_s	full liquid saturation
TCw	Tiva Canyon welded unit at Yucca Mountain
TSw1-2	Topopah Springs welded units at Yucca Mountain
α	van Genuchten fitting parameter (1/Pa)
β	van Genuchten fitting parameter
ρ	liquid density (kg/m^3)
μ	dynamic liquid viscosity (kg/m-sec)

Subscripts:

f   fracture

m   matrix

Acknowledgments

References

Dudley, A.L., R.R. Peters, J.H. Gauthier, M.L. Wilson, M.S. Tierney, and E.A. Klavetter (1988). Total System Performance Assessment Code (TOSPAC) Volume 1: Physical and Mathematical Bases, SAND85-0002, Sandia National Laboratories, Albuquerque, NM.

Glass, R.J. and V.C. Tidwell (1991). Research Program to Develop and Validate Conceptual Models for Flow and Transport Through Unsaturated, Fractured Rock, SAND90-2261, Sandia National Laboratories, Albuquerque, NM.

Klavetter, E.A. and R.R. Peters (1986) Estimation of Hydrologic Properties of an Unsaturated, Fractured Rock Mass, SAND84-2642, Sandia National Laboratories, Albuquerque, NM.

Pruess, K. (1991). TOUGH2–A General-Purpose Numerical Simulator for Multiphase Fluid and Heat Flow, LBL-29400, Lawrence Berkeley Laboratories.

Pruess, K. and T.N. Narasimhan (1985). A Practical Method for Modeling Fluid and Heat Flow in Fractured Porous Media, *Society of Petroleum Engineers Journal*, 25, pp. 14–26.

Pruess, K. (1983). GMINC—A Mesh Generator for Flow Simulations in Fractured Reservoirs, LBL-15227, Lawrence Berkeley Laboratory, Berkeley, CA.

van Genuchten, M.Th. (1980). A Closed-Form Equation for Predicting the Hydraulic Conductivity of Unsaturated Soils, *Soil Sci. Soc. Am. J.*, Vol 44, pp. 892-898.

Wilson, M.L., J.H. Gauthier, R.W. Barnard, G.E. Barr, H.A. Dockery, E. Dunn, R.R. Eaton, D.C. Guerin, N. Lu, M.J. Martinez, R. Nilson, C.A. Rautman, T.H. Robey, B. Ross, E.E. Ryder, A.R. Schenker, S.A. Shannon, L.H. Skinner, W.G. Halsey, J. Gansemer, L.C. Lewis, A.D. Lamont, I.R. Triay, A. Meijer, and D.E. Morris (1994). Total-System Performance Assessment for Yucca Mountain—SNL Second Iteration (TSPA-1993), SAND93-2675, Sandia National Laboratories, Albuquerque, NM.

DISCLAIMER